Published in final edited form as:
Oncogene. 2013 March 21; 32(12): 1497–1507. doi:10.1038/onc.2012.168.

The Grainyhead transcription factor Grhl3/Get1, suppresses miR-21 expression and tumorigenesis in skin: Modulation of the miR-21 target MSH2 by RNA-binding protein DND1

Ambica Bhandari[#,1], **William Gordon**[#,1,2], **Diana Dizon**[1], **Amelia Soto Hopkin**[1], **Elizabeth Gordon**[3,4], **Zhenquan Yu**[1], and **Bogi Andersen**[*,1,2]

[1]Department of Medicine, Department of Biological Chemistry, University of California Irvine, Irvine, CA

[2]Center for Complex Biological Systems, University of California Irvine, Irvine, CA

[3]Department of Development and Cell Biology, University of California Irvine, Irvine, CA

[4]Institute for Genomics and Bioinformatics, University of California, Irvine, CA

Abstract

Epidermal differentiation and stratification, crucial for barrier formation, are regulated by a complex interplay of transcription factors, including the evolutionarily conserved Grainyhead-like 3 (Grhl3/Get1); *Grhl3*-deleted mice exhibit impaired epidermal differentiation and decreased expression of multiple differentiation genes. To test whether Grhl3 regulates epidermal genes indirectly by controlling the expression of specific microRNAs (miRs), we performed miR profiling and identified 11 miRs that are differentially regulated in *Grhl3*-/- skin, one of which is miR-21, previously shown to be upregulated in diseased skin, including in psoriasis and squamous cell skin cancer. We found that miR-21 is normally expressed in the post-mitotic suprabasal layers of the epidermis, overlapping with Grhl3. The miR-21 promoter is bound and repressed by Grhl3 indicating that these two factors are involved in a regulatory loop maintaining homeostasis in the epidermis. While miR-21 overexpression in normal keratinocytes had mild effects on the expression of several known miR-21 targets, an enhanced downregulation of the miR-21 tumor-related targets, including MSH2, was observed in Ras-transformed keratinocytes. The increased sensitivity of transformed keratinocytes to miR-21′s effects occurs in part through downregulation of the RNA-binding protein DND1 during the transformation process. Additionally, we observed increased tumorigenesis in mice subcutaneously injected with transformed keratinocytes lacking *Grhl3*. These findings indicate that decreased Grhl3 expression contributes to tumor progression and upregulation of the oncomir miR-21 in squamous cell carcinoma of the skin.

[*]To whom correspondence should be addressed: Bogi Andersen, Sprague Hall, Room 206, University of California, Irvine, Irvine, CA 92697-4030, bogi@uci.edu, Phone: 949-824-9093.
[#]Denotes equal authorship

Conflict of Interest: The authors have no conflict of interest.

Introduction

The protective multi-layered epidermis undergoes continuous renewal throughout the life of an organism. Its deepest layer, the basal cell layer, consists of proliferating progenitor cells that undergo a series of differentiation steps as they move towards the surface, forming first the spinous layer, then the granular layer, and finally the cornified layer before eventually sloughing off to make space for new cells (1). Disruption of epidermal homeostasis is a prominent feature of many skin diseases, including skin cancer, the most common human malignancy. The homeostatic process is executed through a gene expression program controlled by a battery of transcription factors including Grhl3, Klf4, and Trp63 (1). More recently, a class of novel regulators of mRNA expression called micro(mi)RNAs has been identified as another important source of regulation within this process. The initial recognition of the importance of miRNAs in skin came first from studies of the skin-specific knockouts of Dicer and DGCR8 in mice (2-4). These mice show prominent neonatal lethality and pups that do survive show severe defects in both hair-follicle morphogenesis and epidermal differentiation. Later, the role of specific miRNAs was studied in the context of epidermal maintenance, including miR-203 (3, 5), miR-34a/c, (6), miR-200 and miR-205 (7-10).

Grainyhead-like 3 (Grhl3; also known as Get1), a transcription factor expressed in the differentiated suprabasal layers, plays an important role in epidermal differentiation and barrier formation by regulating multiple genes important for executing the differentiation program in skin (11, 12). These genes encode for structural proteins, lipid metabolizing enzymes and cell-cell adhesion molecules. Although we observed an enrichment of Grhl3 binding sites among the differentially expressed genes in the skin of *Grhl3*$^{-/-}$ mice (12), many lacked conserved Grhl3 binding sites in their proximal promoter (12), prompting us to explore other mechanisms by which Grhl3 might regulate differentiation genes. We thus hypothesized that Grhl3 regulates some of its potential target genes indirectly by modulating expression of microRNAs. To that effect, we performed miRNA profiling experiments using total RNA from back skin of wild type (WT) and *Grhl3*$^{-/-}$ mice. Among the differentially expressed miRNAs we focused our research on miR-21, which is significantly upregulated miRNA in *Grhl3*$^{-/-}$ skin.

miR-21 is one of the most well studied microRNAs, partly because it is consistently up regulated in malignant cells; it was found to be up regulated in several cancers, including breast, lung, stomach, prostate, colon, and pancreatic tumors (13). miR-21 is abundantly expressed in skin (2, 14-17), and is upregulated in pathological conditions such as psoriasis, atopic dermatitis (18-20), and squamous cell carcinoma (SCC) (21), indicative of its potential importance in skin homeostasis. Therefore, it is intriguing that miR-21 is up regulated in *Grhl3* deficient skin, which exhibits impaired differentiation and hyperplasia. In this study, we show that *Grhl3*$^{-/-}$ keratinocytes display enhanced Ras-mediated tumorigenesis, and that downregulation of Grhl3 in transformed keratinocytes contributes to increased expression of miR-21. In addition, we demonstrate that the sensitivity of miR-21 targets is enhanced in transformed cells, possibly due to decreased expression of the RNA-binding protein DND1. Our studies reveal mechanisms that contribute to the over expression

of miR-21 in squamous cell carcinoma and enhanced sensitivity to miR-21 for its targets in malignant keratinocytes.

Results

miRNA expression profiling identifies differentially expressed miRNAs in the skin of Grhl3$^{-/-}$ mice

To test the hypothesis that Grhl3 directly or indirectly regulates the expression of specific miRNAs in the skin, we globally profiled miRNA expression in the dorsal skin of wild type (WT) and *Grhl3*$^{-/-}$ mice at embryonic day (e) 18.5. To decrease false positives, we performed two independent profiling experiments, using a paired approach where both sample types (WT and *Grhl3*$^{-/-}$) were hybridized to the same chip, and a non-paired approach where the two sample types were hybridized to different chips with the same reference pool of RNA (Figure 1a). Using a significance cutoff of $p \leq 0.05$, we identified 44 and 30 differentially expressed miRNAs in the paired and non-paired experiments, respectively (Supplementary Table 1). A total of 11 miRNAs, 6 down-regulated and 5 up-regulated, were identified in both experiments (Table 1). We validated 8 of these differentially expressed miRNAs by quantitative PCR and found that 7 were altered in the same direction as observed in the miRNA profiling experiments (Table 1). These experiments indicate that the loss of Grhl3 leads to alterations in the skin expression of several miRNAs, indicating a link between the transcriptional control of epidermal differentiation and miRNA expression.

Epidermal expression of miR-21 correlates with differentiation

One of the microRNAs overexpressed in e18.5 *Grhl3*$^{-/-}$ mouse skin was miR-21, a microRNA previously shown to be overexpressed in pathological skin (19-21), prompting us to focus our study on the regulation and role of miR-21 in epidermal keratinocytes. We first measured mature miR-21 skin expression during mouse embryogenesis from e14.5 to e18.5, the time period corresponding to critical epidermal differentiation steps (1). miR-21 is expressed highly throughout this period in WT mice and was significantly differentially regulated in Grhl3$^{-/-}$ skin from e15.5 to e18.5 (Figure 1b) correlating with the phenotypic appearance of defective epidermal differentiation in Grhl3$^{-/-}$ mice (12, 28). Up-regulation of miR-21 in *Grhl3*$^{-/-}$ skin was selective to the epidermis where Grhl3 is expressed (Figure 1c). *In-situ* hybridization showed predominant miR-21 expression in the post-mitotic, differentiated suprabasal layers of the epidermis (Figure 1d, Supplemental figure 1), indicating that miR-21′s spatial expression correlates with epidermal differentiation and Grhl3 expression in normal mouse skin. In addition, there is low but clear expression in hair follicles as well as diffuse, low level expression in the basal layer and throughout the dermis. Together these data indicate that in normal epidermis, miR-21 expression correlates with differentiation. Intriguingly, in *Grhl3*-deleted skin, which exhibits impaired differentiation and a barrier defect, there is increased expression of miR-21, suggesting the possibility of a regulatory loop involving Grhl3 and miR-21 in the control of epidermal homeostasis.

Grhl3 binds to and represses the expression of the miR-21 promoter

miR-21 upregulation in *Grhl3*$^{-/-}$ mouse skin, as well as its overlapping expression with Grhl3 in the suprabasal layer of the epidermis, suggests that miR-21 could be a direct Grhl3 target. To test whether miR-21 is differentially regulated at a transcriptional level in the *Grhl3*$^{-/-}$ mouse, we measured expression of its primary transcript (pri-miR21), precursor transcript (pre-miR21), and mature form (miR-21) in both WT and *Grhl3*$^{-/-}$ mouse skin at e16.5. We observed an increase in all three forms of miR-21 in *Grhl3*$^{-/-}$ mouse skin (Figure 2a), suggesting regulation at the level of *miR-21* gene transcription in *Grhl3*$^{-/-}$mice. Since whole mouse skin was used to measure miR-21 expression, we sought to determine if this effect on miR-21 expression was cell autonomous. To test this possibility, we knocked down GRHL3 in cultured normal human keratinocytes (NHEK) by siRNA and induced differentiation with calcium for two days. We then performed quantitative RT-PCR to measure miR-21 levels which were significantly up-regulated (Figure 2b and Supplemental Figure 2a). Conversely we observed a reduction in miR-21 levels when Grhl3 was overexpressed in normal human keratinocytes (Figure 2c and Supplemental Figure 2b). Consistent with these findings, Gene Set Enrichment Analysis (29, 30) on differentially expressed genes in *GRHL3*-knocked down NHEK, as determined by Affymetrix microarray analysis, revealed “regulation by miR-21” as one of the overrepresented categories (Figure 2d). Together, these results indicate that Grhl3 regulates *miR-21* transcription in a cell autonomous manner in normal keratinocytes.

To test whether GRHL3 binds to the *miR-21* promoter, we searched for GRHL3 binding sites (Grhl3 BS) using ConSite (31) and found several high scoring sites in the promoter region of the human *mir21* gene, located approximately 3.5kb upstream of the mature miRNA sequence (32). Using chromatin immunoprecipitation (ChIP) and quantitative PCR, there was enrichment of Grhl3 binding to the predicted site in the promoter region in NHEK while no binding was observed to a region further upstream from the promoter (Figure 2e). To test if the Grhl3 binding site is functional we cloned ~900bp of the human *miR-21* promoter region into a luciferase reporter plasmid and measured luciferase activity in presence of Grhl3 expression vector in HaCaT cells which are immortalized human keratinocytes. Expression of Grhl3 mildly but significantly reduced miR-21 luciferase activity, and this repression was relieved by a non-binding (11) mutation of the Grhl3 binding site (Figure 2f and Supplemental Figure 2c). The above results indicate that GRHL3 directly binds to the *miR-21* proximal promoter, reducing miR-21 expression in epidermal keratinocytes.

miR-21 appears dispensable for normal epidermal differentiation

To investigate if knockdown of miR-21 affects normal epidermal differentiation, we took advantage of antagomirs, small RNA inhibitors that can be injected into mice. Locked Nucleic Acid (LNA) modified antagomirs (25, 33), either against miR-21 or scrambled, were injected subcutaneously in the upper dorsal region of newborn mice daily for 3 days. Despite a clear reduction in miR-21 levels in the skin of these mice (Figure 3a), the histology of the injected dorsal skin appeared normal (Figure 3b) and there were no changes in expression of differentiation markers, Keratin 10 and Involucrin (Figure 3c). Similarly, miR-21 antagomirs had no effect on keratinocyte proliferation as assessed by BrdU

incorporation (Figure 3d). These experiments suggest that miR-21 does not play an important role in epidermal differentiation during normal homeostasis. The caveat is that we may not have achieved a complete epidermal knockdown of miR-21 in these experiments. However, these findings are strengthened by recent miR-21 mouse knockout studies (34) which did not report epidermal abnormalities under normal homeostatic conditions. We therefore hypothesize that miR-21 plays a more important role when skin homeostasis is perturbed. Consistent with this idea, miR-21 skin expression is highly up-regulated after full thickness epidermal punch wounding (Supplementary Figure 2d) and after barrier disruption by wax depilation, which transiently induces epidermal hyperproliferation (data not shown).

Microarray expression analysis reveals potential targets of miR-21 in keratinocytes and increased target sensitivity in transformed keratinocytes

In an attempt to tease out a miR-21 role and to identify the genes targeted by miR-21 in keratinocytes, we performed gene expression profiling experiments in normal human keratinocytes transfected with pre-miR21, miR-21 antagomirs (Lna-21), and scrambled controls for both (Figure 4a, Supplementary Figure 3). Using a differential expression cutoff of 1.2-fold, we identified 1107 genes that were downregulated in pre-miR21 transfected cells and 1582 genes that were upregulated in Lna-21 transfected cells. Among these two gene sets, 249 genes were common, a significant enrichment ($p \leq 0.0001$; chi-squared test), indicating that these are likely miR-21 targets in human keratinocytes. To further increase the confidence in miR-21 target prediction, we overlapped this list with genes predicted to be miR-21 targets by miRNA target prediction programs Targetscan and PicTar (35), thus reducing the list to 70 genes ($p \leq 0.0001$; chi-squared test) (Supplementary Table 2). DAVID (36) identified cell cycle as the most significantly enriched functional category by keyword in the list of 70 genes; there were also several genes in the list associated with DNA repair mechanisms. We then used quantitative RT-PCR to validate select genes of interest (*CKAP2, E2F3*), including previously described miR-21 targets (*MSH2, CDK6, PDCD4, CDC25A*), in HaCaT cells. Interestingly, we found only moderate transcript level changes in response to miR-21 over-expression or knock-down with some previously described targets showing no response (Figure 4b and c).

A recent study found that when miR-21 is overexpressed in mice on a mutant Ras background the frequency of skin papillomas increased and conversely when miR-21 is deleted on the mutant Ras background the skin papilloma frequency reduced dramatically (34). These findings, in conjunction with the facts that miR-21 does not appear to regulate normal skin homeostasis, and that its over-expression and knockdown causes only moderate gene expression changes in normal keratinocytes, suggest the possibility that miR-21 affects its targets more strikingly in transformed than normal keratinocytes. To test this hypothesis, we transformed HaCaT cells with Ras and SV40 vectors (37, 38) (Supplementary Figure 4a). We confirmed the integration of the two transgenes into the genome by PCR and subsequent sequencing (Supplementary Figure 4b and 4c). Consistent with a pro-tumorigenic effect of these oncogenes, we observed a reduction in doubling time in the transformed HaCaT cells (data not shown) and tumor growth three weeks after they were injected into nude mice while unmodified HaCaT cells failed to form tumors (Supplementary Figure 4d). We measured mRNA expression levels of known and putative

miR-21 targets in the transformed cells and observed a greater alteration in their expression with both over-expression (Figure 4d) and knockdown of miR-21 (Figure 4e) with similar efficiency of transfection (Supplementary Figure 5).

Transcripts encoding the DNA mismatch repair gene MSH2, loss of which is known to increase tumor predisposition of skin (39, 40), were significantly down- and up-regulated by pre-miR21 and Lna-21, in transformed keratinocytes. Consistent with this finding, MSH2 protein levels were decreased upon miR-21 expression (Figure 4f) and increased mildly upon knockdown of miR-21 (Figure 4g) in transformed HaCaT cells. Furthermore, MSH2 was dramatically reduced in tumors derived from transformed HaCaT cells, correlating with increasing miR-21 levels (Figure 4h and Supplementary Figure 6). These results indicate that keratinocyte transformation increases miR-21 target sensitivity and that miR-21-mediated downregulation of MSH2 could contribute to increased tumor progression.

The RNA binding protein DND1 modulates sensitivity to miR-21 actions

The heightened sensitivity of miR-21 target mRNAs in transformed compared to unmodified HaCaT cells could be due to the differential expression of molecules capable of inhibiting miR-21 action. We therefore investigated the expression of transcripts for three known RNA binding proteins (RBP), dead end homolog 1 (DND1), Embryonic lethal, abnormal vision, Drosophila-like (ELAVL) 1, and KH-type splicing regulatory protein (KHSRP) 1 in the two cell lines. These RBPs are known to bind to the 3′UTRs of miRNA target genes, preventing miRNA binding and thus inhibiting their action (23, 41). We observed reduced expression of DND1 mRNA but not of ELAVL or KHSRP in the transformed HaCaT cells (Figure 5a), as well as loss of DND1 mRNA and protein in tumors from transformed HaCaT cells (Figure 5b and Supplementary Figure 7a and b). Together, these findings raise the possibility that lower levels of DND1 might explain heightened sensitivity to miR-21 actions in transformed HaCaT cells and consistent with this idea, we found that expression of DND1 in transformed HaCaT cells could interfere with the miR-21-mediated repression of MSH2 (Figure 5c and Supplementary Figure 7c). Conversely, when DND1 was knocked-down in transformed HaCaT cells the transcript levels of MSH2 were reduced, and addition of miR-21 further enhanced this effect (Figure 5d and Supplementary Figure 7d). The 3′UTR of MSH2 contains a predicted DND1 binding site (Figure 5e) (27) suggesting a direct interaction between DND1 protein and MSH2 mRNA. Consistently, an HA antibody pulled down MSH2 mRNA in extracts from HaCaT cells transfected with HA-DND1. This interaction is specific as IgG failed to precipitate MSH2 mRNA in these same cells, and HA-antibody failed to precipitate MSH2 in non-transfected HaCaT cells. Furthermore, the HA antibody did not precipitate KLF4 mRNA from the transfected HaCaT cells (Figure 5f). These data suggest that DND1 interacts directly with MSH2 RNA to alter its sensitivity to miR-21.

Grhl3 expression is decreased in mouse and human epidermal carcinomas

In order to better understand the link between Grhl3 regulation of miR-21 and cancer, we studied the expression of Grhl3 in mouse papillomas and carcinomas derived from the two stage DMBA/TPA model of skin carcinogenesis by immunofluorescence (provided by Dr. S. Yuspa). Papillomas showed normal localization and clear expression of Grhl3 while a marked decrease in the expression of Grhl3 was observed in carcinomas, as well as a more

diffuse appearance to its localization (Figure 6a). This was consistent with GRHL3 expression in human skin squamous cell carcinoma samples where GRHL3 expression was reduced or absent in all tumor samples; lowly expressed nuclear signal was detected in only 4 out of 60 tumors whereas strong nuclear expression was detected in 5 out of 5 normal skin samples (Figure 6b and Supplementary Table 3). Together these data provide evidence for decreased Grhl3 expression in both mouse and human squamous cell skin cancers.

Grhl3 deleted keratinocytes show increased tumorigenesis in mice and miR-21 is highly up-regulated in RAS induced tumorigenesis

In order to study the putative link between Grhl3 expression and tumor formation, we utilized RAS transformation of primary epidermal keratinocytes from WT and *Grhl3*$^{-/-}$ mice in a xenograft mouse model. At 5 weeks post injection *Grhl3*$^{-/-}$ tumors were significantly larger than WT tumors (Figure 7a-c). While the tumors appear similar in histological composition, the knockout tumor shows increased cellular density (Figure 7d and e). Consistent with decreased Grhl3 expression in mouse and human skin carcinomas (Figure 6), Grhl3 transcripts were decreased in tumors from Ras-transformed WT keratinocytes (Figure 7f). Additionally miR-21 was highly up-regulated in the RAS induced tumors and was mildly but significantly increased in KO tumors (Supplementary Figure 8). Consistent with our *in vitro* studies Msh2 levels were significantly lower in *Grhl3*$^{-/-}$ than WT tumors (Figure 7g, h, and i). Together, these data show that Ras transformation decreases Grhl3 levels and that Grhl3 acts to inhibit Ras-mediated epidermal keratinocyte tumorigenesis. Correlating with enhanced tumorigenesis in the absence of Grhl3 are increased miR-21 levels and decreased MSH2 levels.

Discussion

The work in this study suggests a model (Figure 8) for how onocogenic mechanisms interact with the differentiation-promoting transcription factor Grhl3 to regulate epidermal tumorigenesis. We find that Grhl3 expression is decreased both in mouse and human squamous cell carcinomas of the skin (Figure 6). Furthermore, we show that Rastransformation of keratinocytes involves suppression of Grhl3 expression (Figure 7f). Decreased expression of Grhl3 in keratinocytes contributes to up-regulation of miR-21 levels (Figure 1 and Supplementary Figure 8) through direct transcriptional regulation of the miR-21 promoter (Figure 2). This regulation creates a positive feedback loop whereby increased miR-21 levels act to enhance the tumorigenic process through multiple mechanisms (Figure 8) (42). In particular, we find that miR-21 targets the DNA repair gene MSH2 in keratinocytes as has been previously shown in breast cancer cells (43). This process is further amplified through transformation-mediated downregulation of the RNA-binding protein DND1 (23) which leads to enhanced sensitivity of MSH2 transcripts to miR-21 interference (Figure 5); DND1 binds directly to the 3′ UTR of MSH2. Overall this model suggests mechanisms whereby epidermal tumorigenesis is driven by complex feed-forward loops involving down-regulation of Grhl3 and up-regulation of oncomir miR-21. Furthermore, our findings demonstrate that Grhl3 acts to suppress tumorigenesis independent of defective barrier formation or wound healing abnormalities, both of which

have been linked to enhanced tumorigenesis in the DMBA/TPA model; a recent study found enhanced tumorigenesis in this model in *Grhl3*$^{-/-}$ mice (44).

Our data in keratinocytes as well as *in-vivo* suggests that miR-21 does not play an important role in normal epidermal differentiation (Figure 3). This is consistent with recent studies showing that miR-21 overexpression (34) and miR-21 KO mice (34, 45) were viable, fertile and had no apparent skin phenotype. Interestingly when these miR-21 overexpressing mice were crossed with Ras-mutant mice, the frequency of skin papillomas increased, indicating the importance of miR-21 in pathological skin conditions like cancer. Furthermore, skin tumorigenesis was reduced in miR-21 knockout mice after Ras activation and in the chemical carcinogenesis model (34, 45). Our results suggest that one mechanism underlying these effects of miR-21 on skin tumorigenesis is down-regulation of tumor suppressors and DNA repair genes such as MSH2. In addition to MSH2, our gene list of likely miR-21 targets identified several other genes that could contribute to tumorigenesis through cell cycle regulation and DNA repair (Figure 4a; Supplementary Table S2) (17, 46), the predominant processes affected by miR-21 perturbation in keratinocytes.

While we show that Grhl3 can directly suppress miR-21 expression, it is a mild repression suggesting that additional mechanisms are likely to contribute to miR-21 up-regulation after transformation. In fact studies have also identified other factors including AP1 that can also drive up miR-21 in tumors (47), and BMP4 as an inhibitor of miR-21 expression in keratinocytes (17). Furthermore, miR-21 itself was recently shown to target Grhl3 (44), suggesting the possibility of a feed-forward autoregulatory loop between Grhl3 and miR-21.

Although our studies focused on tumorigenesis, similar mechanisms may underlie the pathogenesis of other skin diseases like psoriasis and atopic dermatitis where miR-21 is up-regulated (18-20). In fact, during the epidermal wound response miR-21 appears to take on a pro-migratory role, promoting re-epithelialization (48, 49) and since miR-21 has been shown to also be regulated by Stat3 (50) and Stat3 deficient mice show a defect in re-epithelization when wounded (51, 52) a similar regulatory loop involving Stat3 may exist in epidermal wounding.

In conclusion, we show that the pro-differentiation regulator Grhl3 can affect tumorigenesis independent of defective barrier or wounding. As Grhl3 suppresses miR-21 expression in keratinocytes, decreased expression of Grhl3 during tumorigenesis contributes to increased expression of miR-21 which enhances the tumorigenic process by targeting several genes, including MSH2. In addition to the up-regulation of miR-21 in tumors, miR-21 target sensitivity is enhanced in transformed cells, possibly due to reduced expression of the RNA binding protein DND1.

Materials and methods

miRNA profiling

The quality of the total RNA from mouse skin was verified on Agilent's 2100 Bioanalyzer. Total RNA was labeled with Hy3™ or Hy5™ fluorescent label, using the miRCURY™ LNA Array power labeling kit (Exiqon). For the paired approach, KO was labeled with Hy3

and WT with Hy5 while in case of the non-paired approach, each WT and KO were labeled with Hy3, while the reference sample labeled by Hy5 was a pool of all RNAs combined. The Hy3™-labeled samples and a Hy5™-labeled reference RNA sample were mixed pair-wise and hybridized to the miRCURY™ LNA array version 11.0/12.0 (Exiqon), containing capture probes targeting all miRNAs registered in the miRBASE version 12.0. The hybridization and image analysis was performed by Exiqon. Quantified signals were background corrected and normalized using the global LOWESS (LOcally WEighted Scatterplot Smoothing) algorithm.

In-situ hybridization

In situ hybridizations were performed using methods described previously (22). miR-21 and control sense miR-159 probes (Exiqon) were DIG-labeled and hybridized to paraformaldehyde fixed frozen skin sections at 46°C.

Immunohisochemistry and immunofluorescence

Immunohistochemistry and immunofluorescence were performed as previously described (12). MSH2 (Santa Cruz; N-20) and Grhl3 (12) antibodies were used at 1:200 and 1:500, respectively, overnight at 4°C.

Cell Culture and Transfections

Primary keratinocytes (HekN, Invitrogen) were cultured in Epilife low calcium media and HaCaT cells were cultured in DMEM high glucose/10% FBS. premiR21™ (15-30nM), premiR™ miRNA Precursor Negative Control (Applied Biosystems; 15-30nM), Lna21 (20nM) and Lna Scrambled (Exiqon; 20nM) were transfected using Lipofectamine 2000 (Invitrogen). Media was changed after 16-20hrs and undifferentiated cells were collected after 48hrs. For differentiation, cells were incubated for 2 days with 1.8mM CaCl2. premiR21™/premiR™ and a Dnd1 expression plasmid (23) were co-transfected into HaCaT cells using Lipofectamine 2000 and collected 24 hours later. Dnd1 siRNA (Dharmacon) and premiR21™/premiR™ were co-transfected into HaCaT cellsusing Lipofectamine 2000 and collected 24 hours later. A ~900bp human *miR-21* promoter sequence was cloned into pGL3-basic luciferase vector (Promega). The Grhl3 binding site AACCGGTTT was mutated to ACGCGCTTT by site-directed mutagenesis (QuikChange® Kit, Strategene). HaCaT cells were seeded 24hrs before transfection. Luciferase reporter constructs with pcDNA3-Grhl3 (or control) were co-transfected by Lipofectamine 2000 (Invitrogen). Transfections were normalized to Renilla luciferase as described previously (12). Keratinocytes were differentiated with 1.8mM CaCl2 for two days and luciferase activity was measured on the 3rd day.

Western blot Analysis

HaCaT and HekN cells were lysed in NP-40 lysis buffer (150mM NaCl, 1%NP-40, 50 mM Tris, pH 8.0) with Complete Protease Inhibitor Cocktail Tablets (Roche). 10-50ug of whole protein lysate was run on Nupage 4-12% Bis-Tris gels in MOPS (Invitrogen) and transferred onto PVDF for 1 hr at 4C. Quantitative western was performed using Odyssey infrared

imaging system (Li-Cor). Antibodies used: Msh2 (Santa-Cruz; N-20) and Dnd1 (Santa-Cruz; P-25).

Transformation of HaCaT cells

6μg of pBabe puro H-Ras V12 and pBabe-puro SV40 LT (Addgene) were transfected separately and together into Phoenix™ Ampho cells (Orbigen) using Lipofectamine. Media was changed 24 hrs after transfection and viral supernatant collected the next day. Virus was filtered (45μM filter) and stored at -80°C. For infection, HaCaT cells were plated at ~30% confluency in 6-well plates. The viral infection cocktail was diluted 1/1200 in media with Polybrene (4μg/mL). 750 ng/mL puromycin (Mediatech) was added 24hrs after infection (changed every 3 days) and cells were selected for three weeks. PCR Amplification was performed using Ras/SV40 primers (Table S4) to verify insertion and products were sequenced to verify infection.

Quantitative Real Time PCR for mRNA and miRNA

Total RNA was extracted using Trizol (Invitrogen). cDNA was prepared using High Capacity cDNA kit (Applied Biosystems) and RT-PCR performed using Taqman or Sybr Green (Applied Biosystems) with CFX384 Real-Time PCR Detection System (Biorad Laboratories). GAPDH and RPLP0 were used as endogenous controls for human cells and β-actin for mouse. For miRNA expression, miRNA specific cDNA was made using TaqMan two-step miRNA assays (Applied Biosystems) according to the manufacturer's instructions. Sno202 was used as an internal control for mouse and RNU44 for human (Applied Biosystems).

Chromatin immunoprecipitation assays—For the chromatin immunoprecipitation (ChIP) assays, we followed previously described methods (24). Antibody used was Grhl3 (Lifespan LS-C30200).

In-vivo inhibition of miR-21 using Antagomirs

We used Exiqon's miRCURY LNA™ microRNA Power inhibitor for Lna-21 and a scrambled control (Lna-Scr). Probes had full phosphorothioate backbone and Locked Nucleotide Acid (Lna) modified bases as described (25). 1, 5 or 10 mg/ml of the Lna-21 or Lna-Scr in PBS was injected subcutaneously into the dorsal skin of newborn mice for three days and collected on day four. To measure proliferation, pups were injected with 50ug/gm of 5-Bromo-2′-deoxyuridine (Brdu) (Sigma) one hour before euthanasia.

Epidermal/Dermal Separation, Primary Keratinocyte Isolation, and Ras Transformation

Skin from e18.5 embryos was treated with 2.5 mg/ml Dispase (Stem cell technologies) 50/50 with calcium free media at 4°C overnight. Epidermis was separated from dermis for RNA purification or diced to isolate primary cells (CNT-57, CellNTech). The v-*ras*^{Ha} replication-defective ecotropic retrovirus was prepared as described (26). Titer of virus was ~1×10^7 virus/ml. Keratinocytes were infected at a multiplicity of infection of 2–3 viruses per cell with the v-*ras*^{Ha}.

Nude Mouse Xenografting

Xenografts of Ras transformed primary wild-type or *Grhl3*-/- using growth-factorreduced Matrigel with 1×10^6 cells were performed in Nude mice (J:NU, Jackson).

RNA Immunoprecipitation

RNA immunoprecipitation was performed as described (27). HaCaT cells transfected with DND1-HA were washed in cold PBS, lysed in Polysome lysis buffer, frozen at -80C overnight, thawed and cleared for 10min at 15,000g. A/G beads were prepared with HA or IgG antibody in NT2 buffer. Beads brought up in 800ul NT2 with Vanadyl ribonucleoside complexes, DTT, EDTA, and RNase inhibitor(27). 200ul of cleared lysate was added to beads and incubated at 4C for 4hrs. Beads were washed 5× with cold NT2 with RNase inhibitor (RNase out, Invitrogen). RNA was extracted using Trizol and cDNA was generated as described above. RT-PCR was performed on Labnet Gradient PCR machine using gene specific primers.

Supplementary Material

Refer to Web version on PubMed Central for supplementary material.

Acknowledgments

We thank Stuart Yuspa and Andrew Ryscavage for the gift of mouse papilloma and carcinoma sample and the Ras virus. We also thank Reuven Agami for HA-DND1 expression plasmid. Supported by NIH grant AR44882 and the Irving Weinstein Foundation (to BA); the California Tobacco Related Disease Research Program grant 17DT-0192 (to AB); NIH training program in Systems Biology of Development T32- HD60555 (to WG); National Library of Medicine training grant LM07443 (to EG).

References

1. Koster MI, Roop DR. Mechanisms regulating epithelial stratification. Annu Rev Cell Dev Biol. 2007; 23:93–113. [PubMed: 17489688]
2. Andl T, Murchison EP, Liu F, Zhang Y, Yunta-Gonzalez M, Tobias JW, et al. The miRNA-processing enzyme dicer is essential for the morphogenesis and maintenance of hair follicles. Curr Biol. 2006 May 23; 16(10):1041–1049. [PubMed: 16682203]
3. Yi R, Poy MN, Stoffel M, Fuchs E. A skin microRNA promotes differentiation by repressing ‘stemness’. Nature. 2008 Mar 13; 452(7184):225–229. [PubMed: 18311128]
4. Yi R, Pasolli HA, Landthaler M, Hafner M, Ojo T, Sheridan R, et al. DGCR8-dependent microRNA biogenesis is essential for skin development. Proc Natl Acad Sci U S A. 2009 Jan 13; 106(2):498–502. [PubMed: 19114655]
5. Lena AM, Shalom-Feuerstein R, Rivetti di Val Cervo P, Aberdam D, Knight RA, Melino G, et al. miR-203 represses ‘stemness’ by repressing DeltaNp63. Cell Death Differ. 2008 Jul; 15(7):1187–1195. [PubMed: 18483491]
6. Antonini D, Russo MT, De Rosa L, Gorrese M, Del Vecchio L, Missero C. Transcriptional repression of miR-34 family contributes to p63-mediated cell cycle progression in epidermal cells. J Invest Dermatol. 2010 May; 130(5):1249–1257. [PubMed: 20090763]
7. Gregory PA, Bert AG, Paterson EL, Barry SC, Tsykin A, Farshid G, et al. The miR-200 family and miR-205 regulate epithelial to mesenchymal transition by targeting ZEB1 and SIP1. Nat Cell Biol. 2008 May; 10(5):593–601. [PubMed: 18376396]
8. Korpal M, Lee ES, Hu G, Kang Y. The miR-200 family inhibits epithelial-mesenchymal transition and cancer cell migration by direct targeting of E-cadherin transcriptional repressors ZEB1 and ZEB2. J Biol Chem. 2008 May 30; 283(22):14910–14914. [PubMed: 18411277]

9. Park SM, Gaur AB, Lengyel E, Peter ME. The miR-200 family determines the epithelial phenotype of cancer cells by targeting the E-cadherin repressors ZEB1 and ZEB2. Genes Dev. 2008 Apr 1; 22(7):894–907. [PubMed: 18381893]
10. Christoffersen NR, Silahtaroglu A, Orom UA, Kauppinen S, Lund AH. miR-200b mediates post-transcriptional repression of ZFHX1B. RNA. 2007 Aug; 13(8):1172–1178. [PubMed: 17585049]
11. Ting SB, Caddy J, Hislop N, Wilanowski T, Auden A, Zhao LL, et al. A homolog of Drosophila grainy head is essential for epidermal integrity in mice. Science. 2005 Apr 15; 308(5720):411–413. [PubMed: 15831758]
12. Yu Z, Lin KK, Bhandari A, Spencer JA, Xu X, Wang N, et al. The Grainyhead-like epithelial transactivator Get-1/Grhl3 regulates epidermal terminal differentiation and interacts functionally with LMO4. Dev Biol. 2006 Nov 1; 299(1):122–136. [PubMed: 16949565]
13. Volinia S, Calin GA, Liu CG, Ambs S, Cimmino A, Petrocca F, et al. A microRNA expression signature of human solid tumors defines cancer gene targets. Proc Natl Acad Sci U S A. 2006 Feb 14; 103(7):2257–2261. [PubMed: 16461460]
14. Sonkoly E, Wei T, Pavez Lorie E, Suzuki H, Kato M, Torma H, et al. Protein kinase C-dependent upregulation of miR-203 induces the differentiation of human keratinocytes. J Invest Dermatol. 2010 Jan; 130(1):124–134. [PubMed: 19759552]
15. Hildebrand J, Rutze M, Walz N, Gallinat S, Wenck H, Deppert W, et al. A Comprehensive Analysis of MicroRNA Expression During Human Keratinocyte Differentiation In Vitro and In Vivo. J Invest Dermatol. 2010 Sep 9.
16. Yi R, O'Carroll D, Pasolli HA, Zhang Z, Dietrich FS, Tarakhovsky A, et al. Morphogenesis in skin is governed by discrete sets of differentially expressed microRNAs. Nat Genet. 2006 Mar; 38(3): 356–362. [PubMed: 16462742]
17. Ahmed MI, Mardaryev AN, Lewis CJ, Sharov AA, Botchkareva NV. MicroRNA-21 is an important downstream component of BMP signalling in epidermal keratinocytes. J Cell Sci. 2011 Oct 15;124(Pt 20):3399–3404. [PubMed: 21984808]
18. Joyce CE, Zhou X, Xia J, Ryan C, Thrash B, Menter A, et al. Deep sequencing of small RNAs from human skin reveals major alterations in the psoriasis miRNAome. Hum Mol Genet. 2011 Oct 15; 20(20):4025–4040. [PubMed: 21807764]
19. Sonkoly E, Wei T, Janson PC, Saaf A, Lundeberg L, Tengvall-Linder M, et al. MicroRNAs: novel regulators involved in the pathogenesis of psoriasis? PLoS One. 2007; 2(7):e610. [PubMed: 17622355]
20. Zibert JR, Lovendorf MB, Litman T, Olsen J, Kaczkowski B, Skov L. MicroRNAs and potential target interactions in psoriasis. J Dermatol Sci. 2010 Jun; 58(3):177–185. [PubMed: 20417062]
21. Dziunycz P, Iotzova-Weiss G, Eloranta JJ, Lauchli S, Hafner J, French LE, et al. Squamous cell carcinoma of the skin shows a distinct microRNA profile modulated by UV radiation. J Invest Dermatol. 2010 Nov; 130(11):2686–2689. [PubMed: 20574436]
22. Lin KK, Kumar V, Geyfman M, Chudova D, Ihler AT, Smyth P, et al. Circadian clock genes contribute to the regulation of hair follicle cycling. PLoS Genet. 2009 Jul.5(7):e1000573. [PubMed: 19629164]
23. Kedde M, Strasser MJ, Boldajipour B, Oude Vrielink JA, Slanchev K, le Sage C, et al. RNA-binding protein Dnd1 inhibits microRNA access to target mRNA. Cell. 2007 Dec 28; 131(7): 1273–1286. [PubMed: 18155131]
24. Rabinovich A, Jin VX, Rabinovich R, Xu X, Farnham PJ. E2F in vivo binding specificity: comparison of consensus versus nonconsensus binding sites. Genome Res. 2008 Nov; 18(11): 1763–1777. [PubMed: 18836037]
25. Elmen J, Lindow M, Schutz S, Lawrence M, Petri A, Obad S, et al. LNA-mediated microRNA silencing in non-human primates. Nature. 2008 Apr 17; 452(7189):896–899. [PubMed: 18368051]
26. Roop DR, Lowy DR, Tambourin PE, Strickland J, Harper JR, Balaschak M, et al. An activated Harvey ras oncogene produces benign tumours on mouse epidermal tissue. Nature. 1986 Oct 30; Nov 30; 323(6091):822–824. [PubMed: 2430189]
27. Zhu R, Iacovino M, Mahen E, Kyba M, Matin A. Transcripts that associate with the RNA binding protein, DEAD-END (DND1), in embryonic stem (ES) cells. BMC Mol Biol. 2011; 12:37. [PubMed: 21851623]

28. Ting SB, Caddy J, Wilanowski T, Auden A, Cunningham JM, Elias PM, et al. The epidermis of grhl3-null mice displays altered lipid processing and cellular hyperproliferation. Organogenesis. 2005 Apr; 2(2):33–35. [PubMed: 19521564]
29. Subramanian A, Tamayo P, Mootha VK, Mukherjee S, Ebert BL, Gillette MA, et al. Gene set enrichment analysis: a knowledge-based approach for interpreting genome-wide expression profiles. Proc Natl Acad Sci U S A. 2005 Oct 25; 102(43):15545–15550. [PubMed: 16199517]
30. Mootha VK, Lindgren CM, Eriksson KF, Subramanian A, Sihag S, Lehar J, et al. PGC-1alpha-responsive genes involved in oxidative phosphorylation are coordinately downregulated in human diabetes. Nat Genet. 2003 Jul; 34(3):267–273. [PubMed: 12808457]
31. Sandelin A, Wasserman WW, Lenhard B. ConSite: web-based prediction of regulatory elements using cross-species comparison. Nucleic Acids Res. 2004 Jul 1; 32(Web Server issue):W249–252. [PubMed: 15215389]
32. Fujita S, Ito T, Mizutani T, Minoguchi S, Yamamichi N, Sakurai K, et al. miR-21 Gene expression triggered by AP-1 is sustained through a double-negative feedback mechanism. J Mol Biol. 2008 May 2; 378(3):492–504. [PubMed: 18384814]
33. Krutzfeldt J, Rajewsky N, Braich R, Rajeev KG, Tuschl T, Manoharan M, et al. Silencing of microRNAs in vivo with ‘antagomirs’. Nature. 2005 Dec 1; 438(7068):685–689. [PubMed: 16258535]
34. Hatley ME, Patrick DM, Garcia MR, Richardson JA, Bassel-Duby R, van Rooij E, et al. Modulation of K-Ras-dependent lung tumorigenesis by MicroRNA-21. Cancer Cell. 2010 Sep 14; 18(3):282–293. [PubMed: 20832755]
35. Krek A, Grun D, Poy MN, Wolf R, Rosenberg L, Epstein EJ, et al. Combinatorial microRNA target predictions. Nat Genet. 2005 May; 37(5):495–500. [PubMed: 15806104]
36. Dennis G Jr, Sherman BT, Hosack DA, Yang J, Gao W, Lane HC, et al. DAVID: Database for Annotation, Visualization, and Integrated Discovery. Genome Biol. 2003; 4(5):P3. [PubMed: 12734009]
37. Sheibani N, Rhim JS, Allen-Hoffmann BL. Malignant human papillomavirus type 16-transformed human keratinocytes exhibit altered expression of extracellular matrix glycoproteins. Cancer Res. 1991 Nov 1; 51(21):5967–5975. [PubMed: 1657375]
38. Jiang R, Cabras G, Sheng W, Zeng Y, Ooka T. Synergism of BARF1 with Ras induces malignant transformation in primary primate epithelial cells and human nasopharyngeal epithelial cells. Neoplasia. 2009 Sep; 11(9):964–973. [PubMed: 19724690]
39. Meira LB, Cheo DL, Reis AM, Claij N, Burns DK, te Riele H, et al. Mice defective in the mismatch repair gene Msh2 show increased predisposition to UVB radiation-induced skin cancer. DNA Repair (Amst). 2002 Nov 3; 1(11):929–934. [PubMed: 12531020]
40. Reitmair AH, Redston M, Cai JC, Chuang TC, Bjerknes M, Cheng H, et al. Spontaneous intestinal carcinomas and skin neoplasms in Msh2-deficient mice. Cancer Res. 1996 Aug 15; 56(16):3842–3849. [PubMed: 8706033]
41. Bhattacharyya SN, Habermacher R, Martine U, Closs EI, Filipowicz W. Relief of microRNA-mediated translational repression in human cells subjected to stress. Cell. 2006 Jun 16; 125(6): 1111–1124. [PubMed: 16777601]
42. Selcuklu SD, Donoghue MT, Spillane C. miR-21 as a key regulator of oncogenic processes. Biochem Soc Trans. 2009 Aug; 37(Pt 4):918–925. [PubMed: 19614619]
43. Yu Y, Wang Y, Ren X, Tsuyada A, Li A, Liu LJ, et al. Context-dependent bidirectional regulation of the MutS homolog 2 by transforming growth factor beta contributes to chemoresistance in breast cancer cells. Mol Cancer Res. 2010 Dec; 8(12):1633–1642. [PubMed: 21047769]
44. Darido C, Georgy SR, Wilanowski T, Dworkin S, Auden A, Zhao Q, et al. Targeting of the Tumor Suppressor GRHL3 by a miR-21-Dependent Proto-Oncogenic Network Results in PTEN Loss and Tumorigenesis. Cancer Cell. 2011 Nov 15; 20(5):635–648. [PubMed: 22094257]
45. Ma X, Kumar M, Choudhury SN, Becker Buscaglia LE, Barker JR, Kanakamedala K, et al. Loss of the miR-21 allele elevates the expression of its target genes and reduces tumorigenesis. Proc Natl Acad Sci U S A. 2011 Jun 21; 108(25):10144–10149. [PubMed: 21646541]
46. Wang Y, Lee CG. MicroRNA and cancer--focus on apoptosis. J Cell Mol Med. 2009 Jan; 13(1): 12–23. [PubMed: 19175697]

47. Ribas J, Lupold SE. The transcriptional regulation of miR-21, its multiple transcripts, and their implication in prostate cancer. Cell Cycle. 2010 Mar 1; 9(5):923–929. [PubMed: 20160498]

48. Cottonham CL, Kaneko S, Xu L. miR-21 and miR-31 converge on TIAM1 to regulate migration and invasion of colon carcinoma cells. J Biol Chem. 2010 Nov 12; 285(46):35293–35302. [PubMed: 20826792]

49. Yang X, Wang J, Guo SL, Fan KJ, Li J, Wang YL, et al. miR-21 promotes keratinocyte migration and re-epithelialization during wound healing. Int J Biol Sci. 2011; 7(5):685–690. [PubMed: 21647251]

50. Iliopoulos D, Jaeger SA, Hirsch HA, Bulyk ML, Struhl K. STAT3 activation of miR-21 and miR-181b-1 via PTEN and CYLD are part of the epigenetic switch linking inflammation to cancer. Mol Cell. Aug 27; 39(4):493–506. [PubMed: 20797623]

51. Sano S, Itami S, Takeda K, Tarutani M, Yamaguchi Y, Miura H, et al. Keratinocyte-specific ablation of Stat3 exhibits impaired skin remodeling, but does not affect skin morphogenesis. Embo J. 1999 Sep 1; 18(17):4657–4668. [PubMed: 10469645]

52. Kira M, Sano S, Takagi S, Yoshikawa K, Takeda J, Itami S. STAT3 deficiency in keratinocytes leads to compromised cell migration through hyperphosphorylation of p130(cas). J Biol Chem. 2002 Apr 12; 277(15):12931–12936. [PubMed: 11812786]

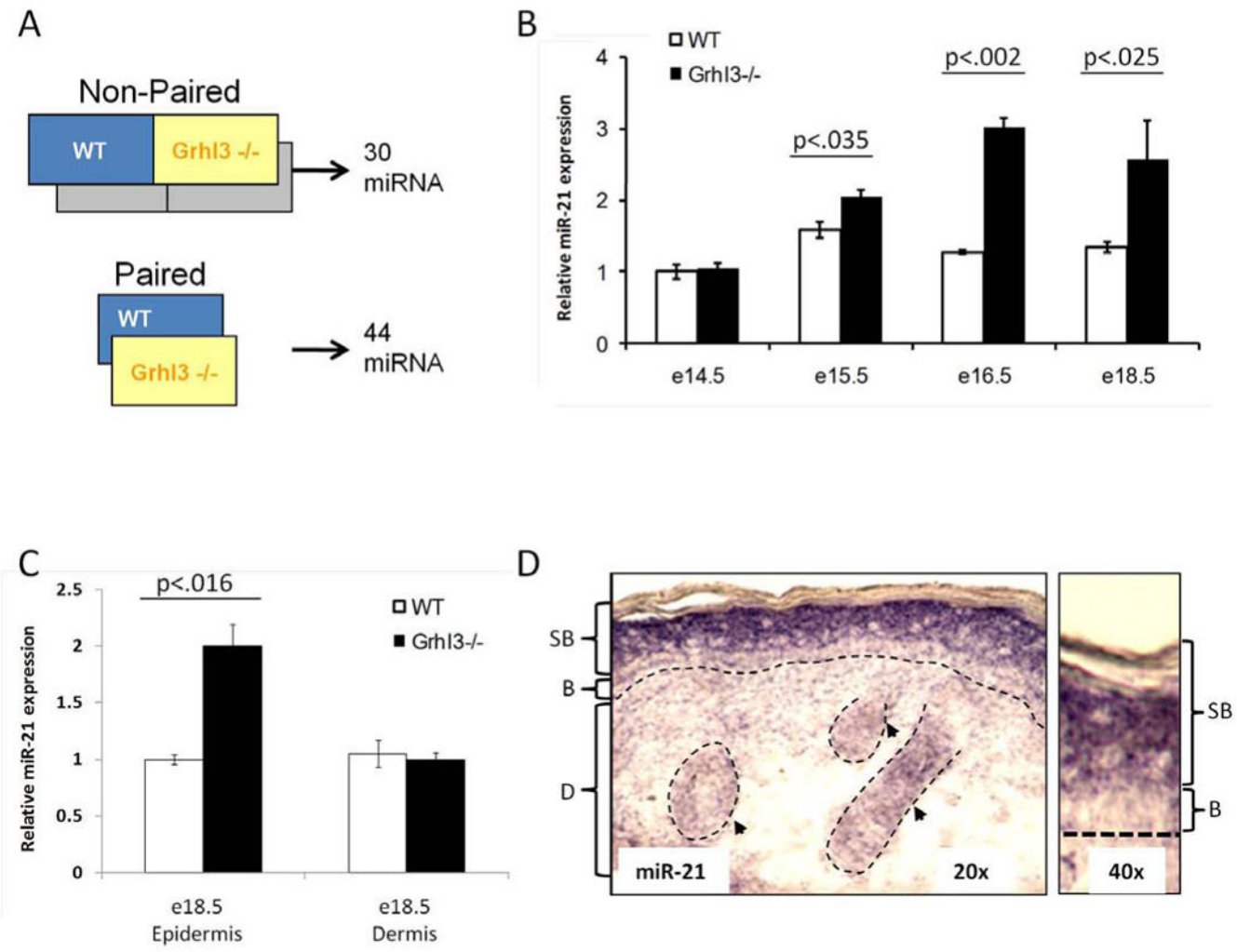

Figure 1. miR-21 is expressed in the suprabasal compartment of the epidermis and its expression increases in *Grhl3*$^{-/-}$ mouse skin

a) Schematic representation of microRNA profiling experiments of *Grhl3*$^{-/-}$ skin, using paired and non-paired hybridization approaches. b) Mature miR-21 expression in skin of wild type (WT) and *Grhl3*$^{-/-}$ mice during the indicated developmental time points. c) Mature miR-21 expression in separated epidermis and dermis from WT and Grhl3$^{-/-}$ mice at e18.5. d) miR-21 expression in mouse epidermis at e18.5 as detected by i*n-situ* hybridization. The broken line traces the basal membrane and outlines the hair follicles. Arrows point to hair follicles (right panel shows epidermis at higher magnification).

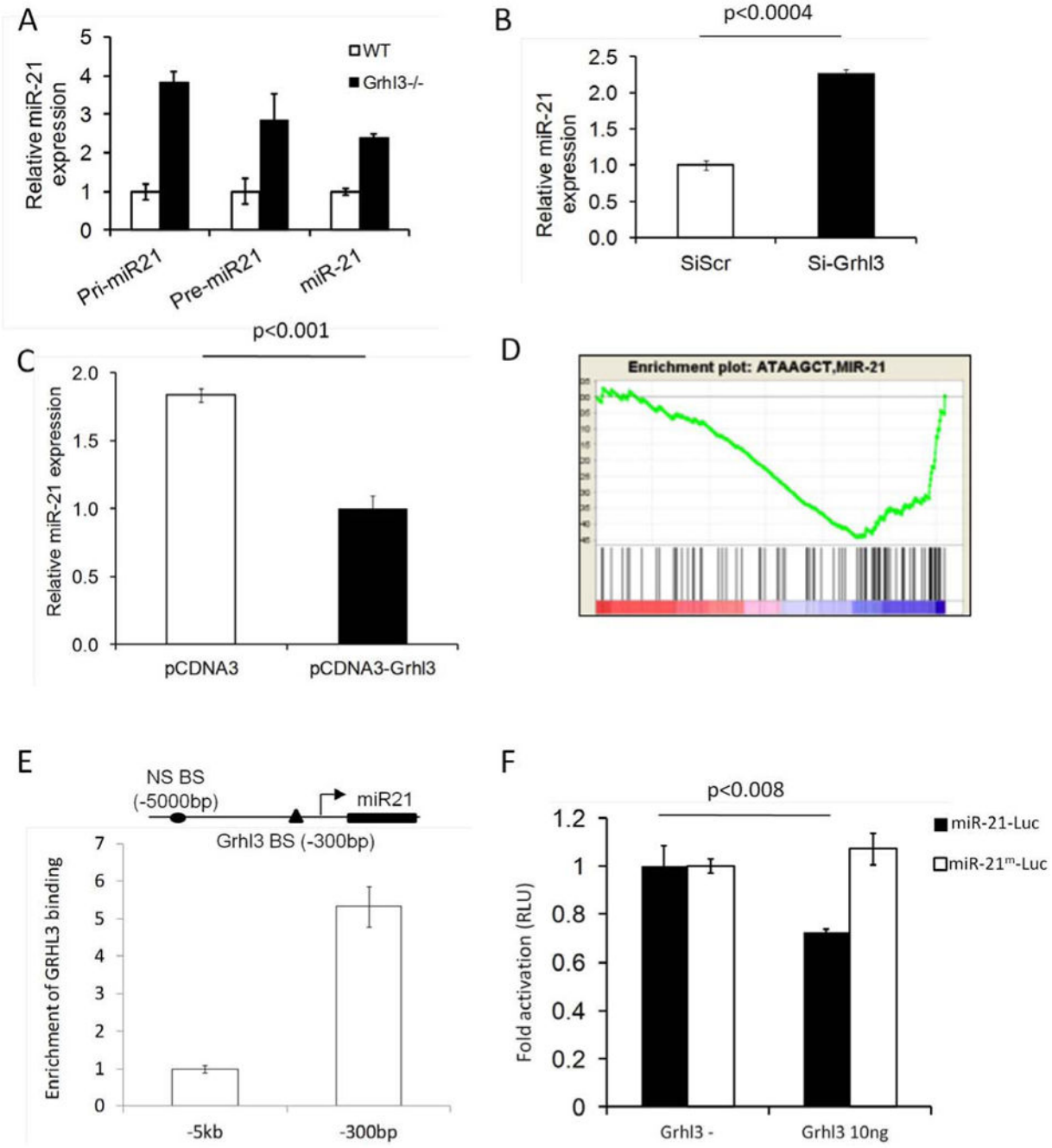

Figure 2. Grhl3 binds to the miR-21 promoter and represses its expression

a) Expression of primary (Pri-miR21), precursor (Pre-miR21) and mature miR-21 was measured by quantitative real-time (qRT) PCR in wild type (WT) and *Grhl3*$^{-/-}$ mouse skin at embryonic day 16.5. b) Normal human keratinocytes were transfected with scrambled (Si-Scr) or Grhl3 (Si-Grhl3) siRNAs and miR-21 expression was measured by qRT-PCR. c) Normal human keratinocytes were transfected with an empty (pcDNA3) or Grhl3 (pcDNA3-Grhl3) expression plasmids and miR-21 expression was measured by qRT-PCR. d) Differentially expressed genes from normal human keratinocytes transfected with Grhl3

siRNA were analyzed with Gene Set Enrichment Analysis, identifying an overrepresentation of miR-21 targets that were up-regulated by Grhl3 knockdown. e) Chromatin immunoprecipitation followed by quantitative PCR. Shown is PCR of Grhl3 immunoprecipitated material with primers from the miR-21 promoter region flanking the predicted Grhl3 binding site (Grhl3 BS) as well as a region lacking binding sites (NS), normalized to IgG non-specific control and input. f) miR-21 reporter plasmid (miR21-Luc) or a miR-21 reporter plasmid in which Grhl3 site is mutated (miR21^{m}-Luc) were transfected into keratinocytes with (10 ng) and without (-) a Grhl3 expression vector. Shown is relative luciferase activity normalized to Renilla.

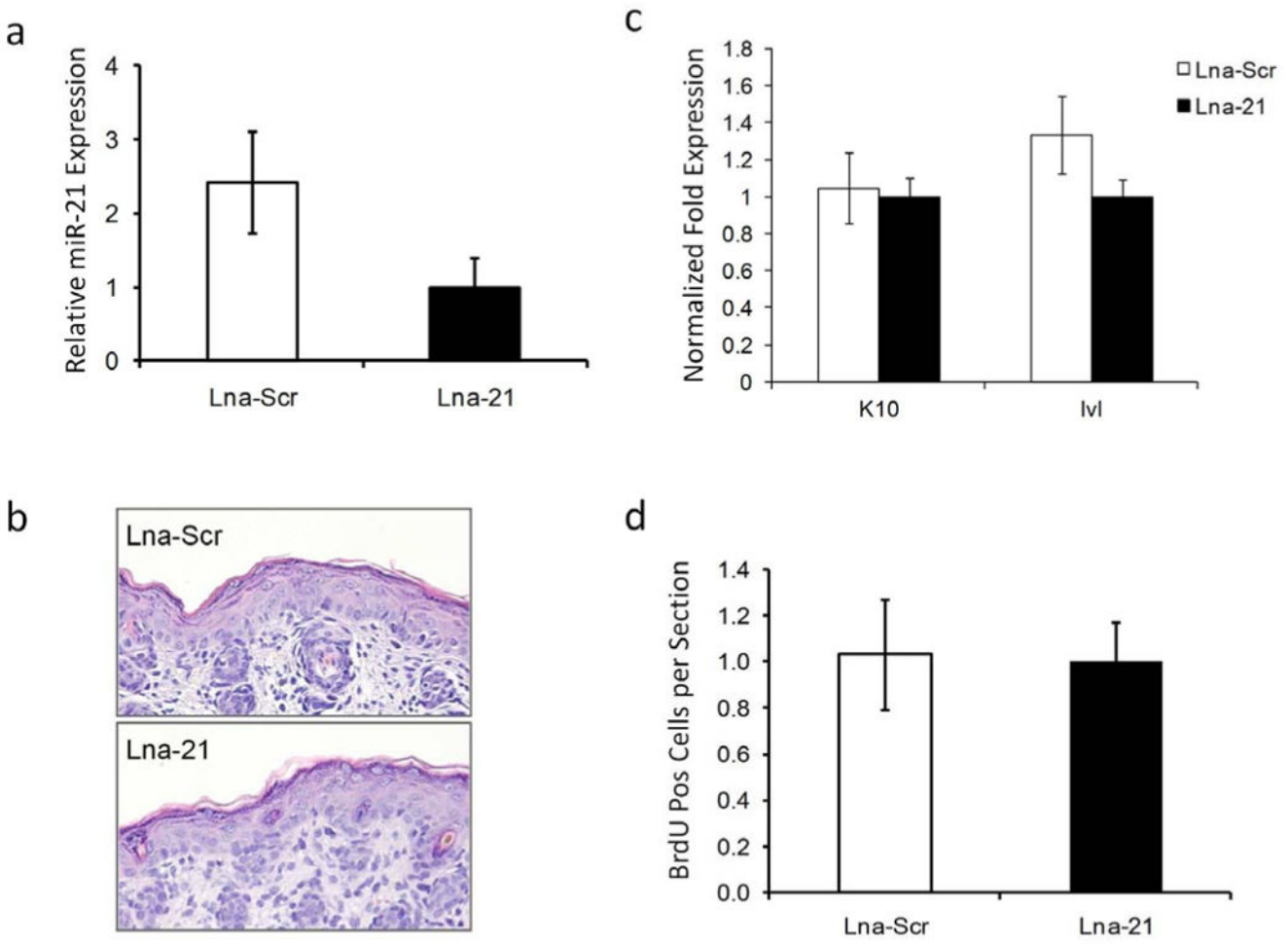

Figure 3. *In-vivo* knockdown of miR-21 does not alter epidermal differentiation or proliferation

a) qRT-PCR of miR-21 levels in dorsal neonatal mouse skin after treatment with scrambled (Lna-Scr) and LNA antagomir of miR-21 (Lna-21). b) Hematoxylin and Eosin stained section of mouse dorsal back skin after treatment with Lna-Scr and Lna-21. c) qRT-PCR showing expression of keratin 10 (K10) and involucrin (Ivl) in dorsal mouse skin after treatment with Lna-Scr and Lna-21. d) Quantification of BrdU-positive cells in mouse skin injected with Lna-Scr and Lna-21.

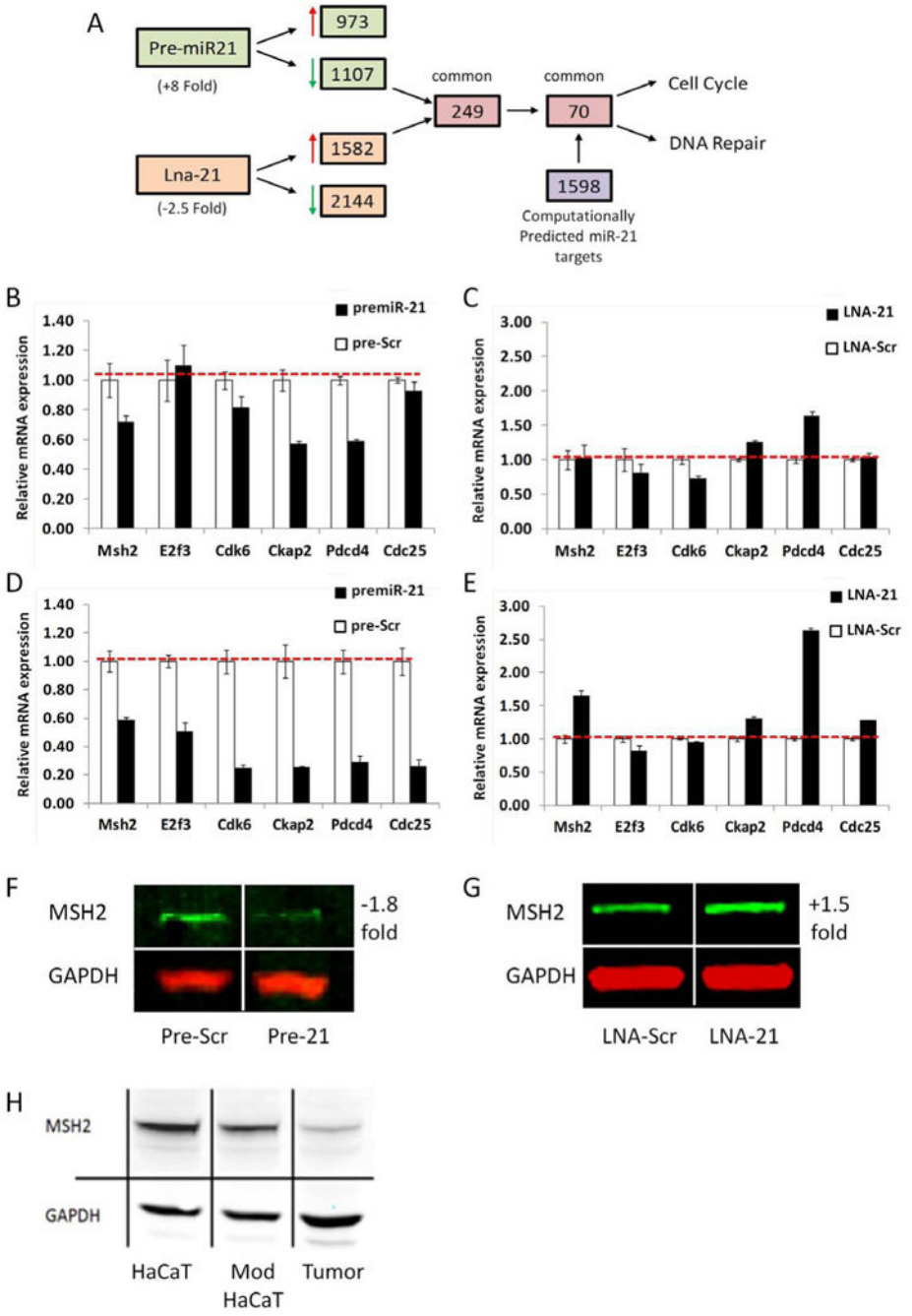

Figure 4. miR-21 regulates MSH2 and other targets more robustly after transformation of keratinocytes

a) miR-21 was over expressed (Pre-miR21) or knocked down (Lna-21) in normal epidermal keratinocytes followed by gene expression microarray analysis. In addition, predicted targets were identified computationally with Targetscan and miRanda. The flow diagram shows the number of genes identified by each method and the overlap of the gene lists. b) qRT-PCR was performed for the indicated genes after transfection with scrambled (Pre-Scr) or miR-21 (Pre-21) into HaCaT cells. c) qRT-PCR was performed for the indicated genes after transfection with scrambled (Lna-Scr) or LNA miR-21 antagomir (Lna-21) into HaCaT

cells. d) qRT-PCR was performed for the indicated genes after transfection with scrambled (Pre-Scr) or miR-21 (Pre-21) into H-Ras/SV40LT-modified HaCaT cells. e) qRT-PCR was performed for the indicated genes after transfection with scrambled (Lna-Scr) or LNA miR-21 antagomir (Lna-21) into H-Ras/SV40LT-modified HaCaT cells. f) Modified HaCaT cells transfected with scrambled (Pre-Scr) or miR-21 (Pre-21) and blotted for MSH2, with GAPDH loading control. Quantification was performed using LICOR and IKK method. g) Modified HaCaT cells were transfected with LNA-Scrambled or LNA miR-21 and blotted for MSH2, with GAPDH loading control. Quantificaton was performed using LICOR and IKK method. h) Quantitative western blot of MSH2 in extracts from HaCaT cells, H-Ras/SV40LT-modified HaCaT cells and tumors derived from H-Ras/SV40LT-modified HaCaT cells, with GAPDH loading control.

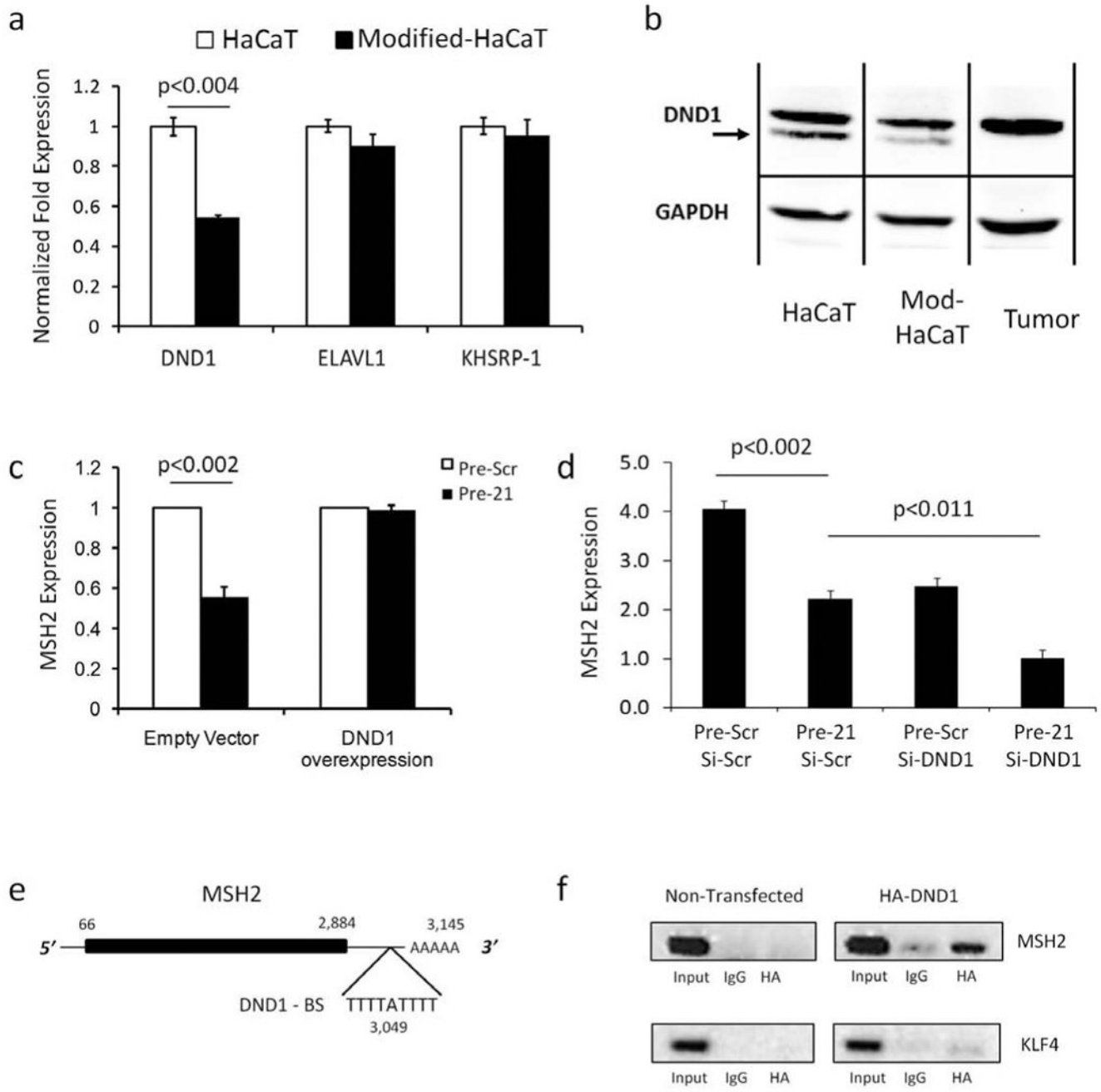

Figure 5. RNA-binding protein DND-1 modulates the sensitivity of MSH2 to miR-21 targeting

a) qRT-PCR analysis of the transcripts encoding the indicated RNA binding proteins in HaCaT and H-Ras/SV40LT-modified HaCaT cells. b) Quantitative western blot of DND1 in extracts from HaCaT, H-Ras/SV40LT-modified HaCaT cells, and tumors derived from modified HaCaT cells (arrow points to DND1 band of appropriate size). GAPDH was probed as a loading control. c) qRT-PCR analysis of MSH2 expression in H-Ras/SV40LT-modified HaCaT cells transfected with scrambled (Pre-Scr) or miR-21 (Pre-mir21), with or without an expression plasmid encoding DND1. d) qRT-PCR analysis of MSH2 expression in H-Ras/SV40LT-modified HaCaT cells transfected with scrambled (Pre-Scr) or miR-21

(Pre-mir21), with or without a DND1 siRNA. e) A schematic of the MSH2 mRNA showing the predicted DND1 binding site (BS) in the 3′ untranslated region (numbers refer to nucleotides from the start of the mRNA). f) RNA immunoprecipitation experiment. HaCaT cells were either not transfected (left panels) or transfected with HA-DND1 (right panels). IP was performed using antibodies against HA or IgG. RNA was purified and MSH2 and KLF4 mRNAs were detected by RT-PCR. RT-PCR on input RNA was included as a control.

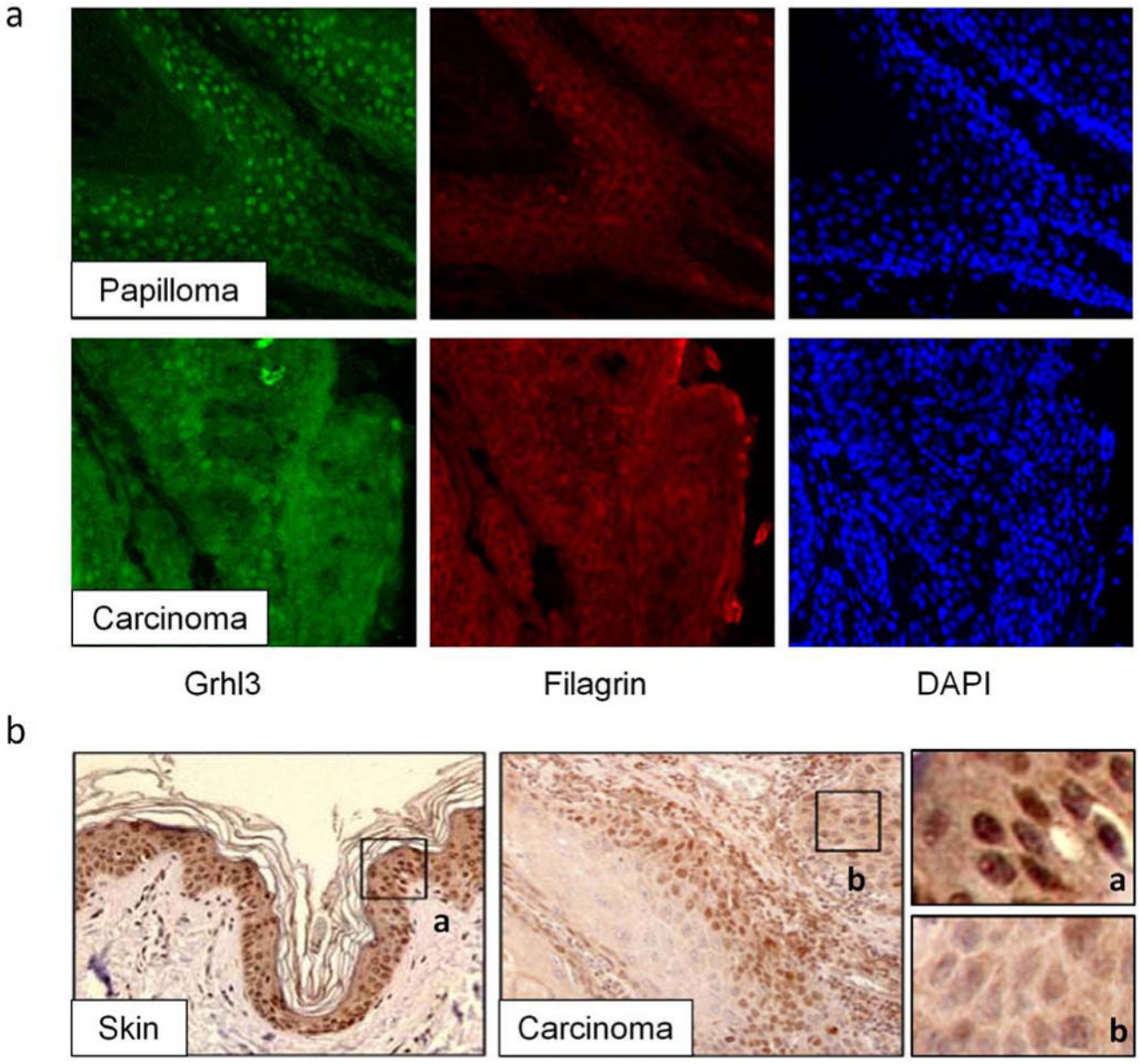

Figure 6. Grainyhead-like 3 expression is reduced in both mouse and human skin squamous cell carcinomas

a) Immuno-fluorescence detection of Grhl3 and Filagrin in mouse papillomas (upper panels) and squamous cell carcinomas (lower panels) derived from the two stage DMBA/TPA model of skin carcinogenesis. b) Immunohistochemical detection of Grhl3 in human normal skin (left panel) and squamous cell carcinoma (middle panel). Higher magnification of normal and squamous cell carcinoma (right panels)

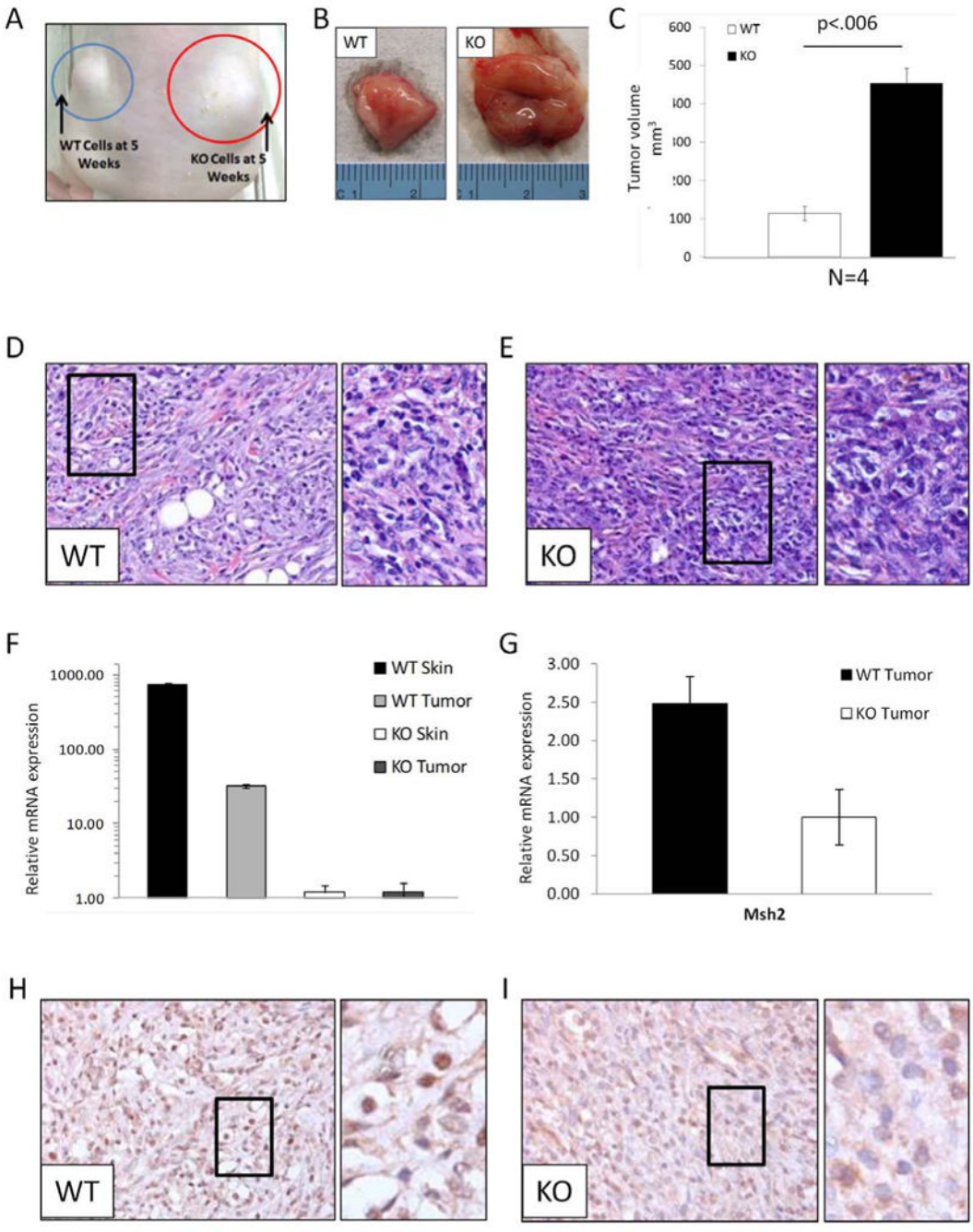

Figure 7. Loss of Grhl3 in mouse epidermal keratinocytes leads to enhanced RAS-mediated tumorigenesis

a) RAS-transformed subcutaneous tumors from keratinocytes derived from WT and *Grhl3*$^{-/-}$ mice (KO). b) Size of representative dissected tumors. c) Average size measurements of four WT and *Grhl3*$^{-/-}$ Ras transformed tumors using following equation, $1/2(LxW)^2$. d-e) Hematoxylin and Eosin stained sections from wild type(d) and KO(e) tumors (inserts show higher magnification). f) qRT-PCR of Grhl3 in mouse skin and tumors derived from transformed keratinocytes. g) qRT-PCR of Msh2 in RAS transformed tumors derived from

wild type and *Grhl3*$^{-/-}$ (KO) keratinocytes. h) Immunohistochemical detection of MSH2 in RAS-transformed tumors from wild type keratinocytes. Insert shows higher magnification. i) Immunohistochemical detection of MSH2 in RAS-transformed tumors from *Grhl3*$^{-/-}$ (KO) keratinocytes. Insert shows higher magnification.

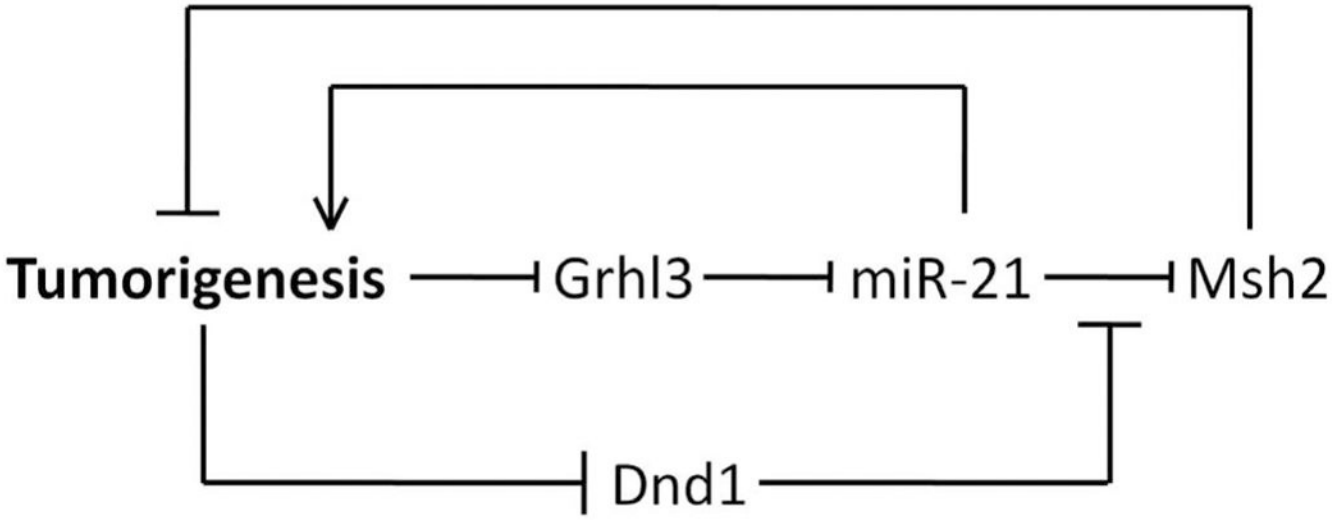

Figure 8. Model of interactions between Grhl3 and miR-21 in skin tumorigenesis

Transformation decreases the expression of Grhl3 which leads to up-regulation of miR-21 as Grhl3 normally binds to the miR-21 promoter and represses its expression. Increased miR-21 levels lead to a decrease in the expression of Msh2 as well as other tumor suppressor targets, thus further promoting tumorigenesis. The RNA binding protein DND1, which decreases the miR-21 target sensitivity of MSH2, is downregulated in tumorigenesis thereby increasing the effectiveness of miR-21 in tumors.

Table 1

Differentially regulated microRNAs in Grhl3 -/- Skin common to two approaches

	Non-paired		Paired		qPCR-Validation
MicroRNA	**P-value**	**Fold**	**P-value**	**Fold**	**KO/WT ± SEM**
mmu-miR-133b	0.0003	-1.4	0.043	-1.3	-1.4 ± 0.16
mmu-miR-133a	0.0002	-1.4	0.049	-1.4	-1.26 ± 0.24
mmu-miR-673-5p	0.005	-1.3	0.012	-1.4	ND
mmu-miR-712	0.008	-1.3	0.002	-1.8	ND
mmu-miR-431	0.007	-1.3	0.042	-1.3	-1.6 ± 0.13
mmu-miR-299*	0.031	-1.2	0.007	-1.5	1.06 ± 0.43
mmu-miR-29b	0.005	1.5	0.001	2.3	2 ± 0.5
mmu-miR-21	0.001	1.5	0.001	2.2	2.5 ± 0.6
mmu-miR-142-3p	0.004	1.5	0.036	2.3	ND
mmu-miR-706	0.006	1.6	0.005	1.4	1.96 ± 0.36
mmu-miR-142-5p	0.002	1.6	0.029	2.1	2.09 ± 0.19